Figure 2. Analytical fluorescence curves of (A) rhodamine 6G in ultrapure water with photomultiplier voltage at 1250 V; (B) rhodamine 6G in purified ethanol at 1200 V; and (C) aflatoxin B_1 and G_1 (1:1) in purified ethanol at 1250 V. The straight lines are best least-squares fits. The error bars on the data points represent estimates based on the fluctuations in the signal level. Note that the slope in (C) is flatter than in (A) although the same photomultiplier voltage setting is used. This is a consequence of the fact that the quantum yield of aflatoxin is less than that of rhodamine 6G.

transmitted by the filters. However, this difficulty can be removed by an improvement in the cell design and filter system, allowing the detection limits to be extended still further. These results encourage us to believe that in many diverse situations requiring ultrasensitivity, laser fluorimetry can reduce the limits of detection by several orders of magnitude.

References and Notes

(1) J. D. Winefordner, S. G. Schulman, and T. C. O'Haver, "Luminescence Spectroscopy in Analytical Chemistry", Wiley-Interscience, New York, N.Y., 1972.
(2) R. N. Zare and P. J. Dagdigian, Science, 185, 739 (1974).
(3) See "Fluorometry Reviews", G.K. Turner, Palo Alto, Calif., 1968, pp 1–19.
(4) L. A. Goldblatt, "Aflatoxin, Scientific Background, Control and Implications", Academic Press, New York, N.Y., 1969.
(5) K. H. Drexhage, "Topics in Applied Physics", Vol. 1, F. P. Schäfer, Ed., Springer-Verlag, Berlin, 1973, pp 144–274.
(6) G. C. Guilbault, "Practical Fluorescence", Marcel Dekker, New York, N.Y., 1973, p 292.
(7) C. A. Parker, "Photoluminescence of Solutions", Elsevier Amsterdam, 1968, p 421.
(8) B. B. Snavely and F. P. Schäfer, Phys. Lett. A, 28, 728–729 (1969).
(9) M. R. Berman and R. N. Zare, Anal. Chem., 47, 1200–1201 (1975).

A. Beatrice Bradley, Richard N. Zare*
*Department of Chemistry, Columbia University
New York, New York 10027*

maximum occurs at 555 nm.[6] Aflatoxin B_1 and G_1 (1:1 mixture) is obtained from Dr. L. M. Seitz (U.S. Grain Marketing Research Center, Manhattan, Kan.).

The sample cell and all glassware were soaked in concentrated nitric acid, rinsed with hydrofluoric acid, and washed amply with solvent and sample. The strong background fluorescence of solvent impurities, when exposed to laser light, was considerably reduced by purification of the solvents. Absolute ethanol was obtained by fractional distillation,[7] and ultrapure water was obtained using four filters, two deionizing tanks, two carbon tanks, followed by all-glass distillation. The dye solutions were not deoxygenated; however, the effect of dissolved oxygen on rhodamine 6G is mainly to depopulate triplet states.[8]

Figure 2 shows the dependence of the fluorescence signal on concentration for rhodamine 6G in water (Figure 2A), rhodamine 6G in ethanol (Figure 2B), and aflatoxin B_1 and G_1 (1:1) in ethanol (Figure 2C). An upper limit to the linearity for the dye solutions occurs at 2×10^{-6} M, where self-quenching and reabsorption of the luminescence causes nonlinearities. For low concentrations, the limit of detection of rhodamine 6G in water is 1.3×10^{-12} M (0.62 parts per trillion) and in ethanol 8.2×10^{-13} M (0.39 parts per trillion). For the aflatoxin solution the limit of detection is 7.8×10^{-12} M (2.5 parts per trillion). Since the laser, when focused on the sample cell, excites molecules only in about 0.6 ml of the total volume, the given detection limit implies that 3×10^8 dye molecules in solution are being detected by the present technique. This limit also corresponds to 1.7 pg of aflatoxin in the volume excited. This appears to be the smallest quantity of aflatoxin yet detected.[4,9] Even so, we have not attempted here to take advantage of the coherence properties of the laser beam, which permit it to be focused to a diffraction-limited spot, facilitating the use of laser fluorimetry in microanalysis.

At present, the major background interference arises from residual light scattered by the sample cuvette and

Thermodynamics of Exciplex Formation by Time-Resolved Nanosecond Flash Spectroscopy

Sir:

We have recently proved[1] the intermediacy of singlet exciplexes in several [2 + 2] photocycloadditions to the phenanthrene chromophore. A complete understanding of both exciplex formation and decay is now clearly implicit to an understanding of many bimolecular photochemical reactions. One important aspect of exciplex decay, reversibility of the formation step, is relatively unexplored. Weller[2] has determined thermodynamic parameters[3,4] in the formation of arene–amine exciplexes, where reversion sometimes dominates other processes of exciplex decay. The negative temperature dependence of several photocycloadditions has been attributed to the reversibility of exciplex formation;[5] however, in these cases complete kinetic analysis was precluded by the lack of exciplex emission. We now present the results of a time-resolved spectrofluorimetric study which leads to an essentially complete analysis of photoreactions involving reversibly formed, emitting exciplexes. Photophysical and thermodynamic parameters are similar for reactive and nonreactive[2] exciplexes. The major difference between the two thus seems no more than the presence of reactive exit channels in the former.

We have utilized a pulsed nitrogen laser (3371 Å, full width at half maximum, FWHM, $\simeq 8$ ns), a PAR 162 boxcar integrator equipped with a Model 164 processor module (aperture 5 ns), and a Spex 1704 monochromator equipped with either an RCA 1P28 or a Hamamatsu R446 photomultiplier. The time–constant of the Model 164 processor is ca. 9 ns and hence the laser pulse convoluted with the boxcar response has a FWHM of ca. 15 ns. The boxcar aperture delay could be scanned (mode I) leading to a time pro-

Table I. Kinetic and Thermodynamic Parameters for Exciplexes[a]

	Σk^C $(s^{-1})^e$	$\phi_F{}^f$	$k_F{}^C$ (s^{-1})	$\phi_R{}^g$	$k_R{}^C$ (s^{-1})	K_{eq} $(M^{-1})^f$	k_{CM} $(M^{-1} s^{-1})$	k_{MC} (s^{-1})	$\frac{(k_{IS}{}^C + k_D{}^C)}{(s^{-1})^i}$
Anth···DEA[b]	9.1×10^6	0.60	5.45×10^6	~0	~0	9.2×10^3	9.2×10^9	1.0×10^6	3.65×10^6
Phen···FN[c]	5.1×10^7	0.049	2.5×10^6	<0.001	$<5 \times 10^4$	6.6×10^2	1.55×10^{10}	2.4×10^7	4.8×10^7
9CNP···p-BA[d]	3.0×10^7	0.14	4.2×10^6	0.07^h	2.1×10^6	3.7×10^2	4.1×10^9	1.1×10^7	2.4×10^7
9CNP···t-A	1.1×10^8	0.038	4.0×10^6	0.4^h	4.2×10^7	1.26×10^2	6.6×10^9	5.7×10^7	6.4×10^7
				$\Delta G°{}^j$	$T\Delta S°{}^{jk}$	$\Delta H°{}^j$	$E_R{}^j$		
Anth···DEA				−5.4	(−4.5)	-9.9^l	7.7		
Phen···FN				−3.8	(−4.5)	-8.3^l	11.4		
9CNP···p-BA				−3.5	−3.9	−7.4	9.45		
9CNP···t-A				−2.8	(−4.5)	-7.3^l	7.6		

[a] Outgassed benzene. [b] Anthracene···diethylaniline. [c] Phenanthrene···fumaronitrile. [d] 9-Cyanophenanthrene···p-butenylanisole. [e] $\Sigma k^C = 1/\tau_C$; τ_C measured in mode I experiments. [f] Precision ±10%. [g] Quantum yields for photoaddition to the arene. [h] R. A. Caldwell and L. Smith, *J. Am. Chem. Soc.*, 96, 2994 (1974). [i] $k_{IS}{}^C + k_D{}^C = \Sigma k^C - (k_R{}^C + k_F{}^C)$. [j] kcal mol^{-1}. [k] At 300 K. [l] Calculated assuming $\Delta S° \approx -15$ cal deg^{-1} mol^{-1}.
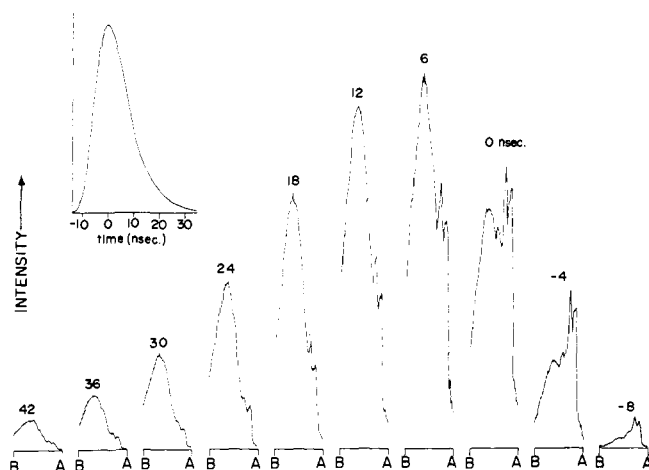

Figure 1. Time-resolved emission spectra in the system 9CNP···t-A. Spectra were recorded from 340 nm (A) to 490 nm (B) at times (t) before and after the peak (l = 0 ns) of the N₂ laser pulse. Inset: laser pulse profile as function of t.

Figure 2. (A) Corrected time-resolved emission spectrum at $t = 36$ ns for the system 9CNP···t-A. (B) 9CNP contribution to total spectrum. (C) Exciplex contribution to total spectrum.

file of emission at a particular wavelength; alternatively, by maintaining a constant delay time, and recording the output as a function of wavelength (mode II), the emission spectrum of the system at a particular time following the laser pulse could be presented. A repetition rate of 20 s^{-1} allowed ca. 200 pulses per nanometer in mode II. The time base was calibrated with a 50-MHz quartz crystal oscillator and standard deconvolution techniques afforded lifetimes in good agreement with those expected for degassed phenanthrene (59.1 ns vs. 60 ns expected[6]) and 10^{-3} M aerated anthracene (3.7 ns vs. 4.0 ns expected[7]).

Figure 1 shows a mode II experiment for the system 9-cyanophenanthrene (9CNP)-*trans*-anethole (t-A) in outgassed benzene, the experimentally most difficult case we have studied in that the exciplex and (quenched) monomer lifetimes were shortest. The expected lifetime of 9CNP in this experiment is ca. 1.0 ns and >99.99% of the initially excited monomer will thus have been quenched at $t \gtrsim 40$ ns. The ratio of the 9CNP (λ_{max} 378 nm) to exciplex (λ_{max} 450 nm) emission does not go to zero, however, but remains constant for $t \gtrsim 35$ ns.[8] This behavior is to be expected[3b,4] when *the emitting species do not decay independently*. The shape of the expanded and corrected spectru below about 370 nm (i.e., throughout the monomer 0 fluorescence band) is essentially free of complex emissi 1 (Figure 2). The monomer contribution can therefore be subtracted from the total spectrum and I_C/I_M, the fluorescence yield ratio of exciplex to monomer in the stationary ratio region, readily calculated.
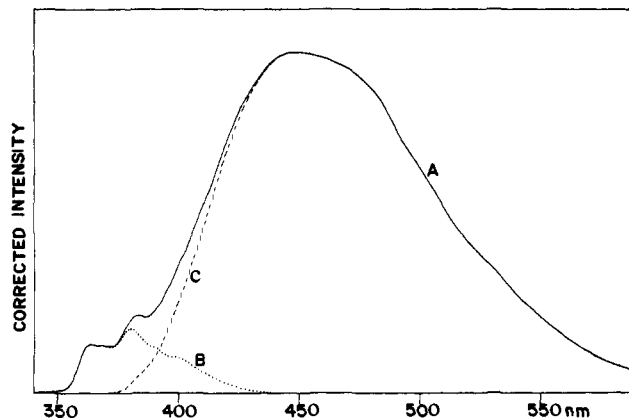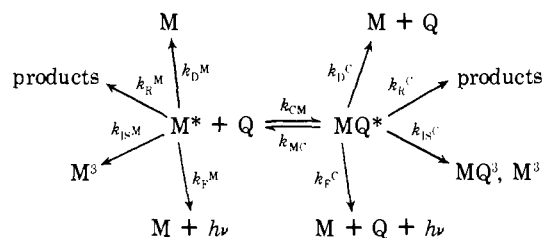
From the partial kinetic scheme (Scheme I) given below

Scheme I

(using Steven's notation[4]) the equilibrium constant $K_{eq} = k_{CM}/k_{MC}$ can be determined.

The equation below may be derived for the stationary ratio portion of the curve from the relationship

$$\frac{1}{[M^*]}\frac{d[M^*]}{dt} = \frac{1}{[MQ^*]}\frac{d[MQ^*]}{dt}$$

(i.e., the operational definition of a stationary ratio), the general expressions for $d[M^*]/dt$ and $d[MQ^*]/dt$ implied by the scheme, and the continuous irradiation Stern-Volmer slope $S = k_{CM}\tau_M/(1 + k_{MC}\tau_C)$ for quenching of M* by Q. The derivation will be presented in the full paper.

$$K_{eq} = \frac{uS(u + \tau_C/\tau_M)}{(u + 1)S[Q] - u(\tau_M/\tau_C - 1)}$$

wh₁ ₂

$$u = \frac{[MQ^*]}{[M^*]} = \frac{\phi_F{}^M}{\phi_F{}^C} \times \frac{\tau_C}{\tau_M} \times \frac{I_C}{I_M}$$

is the experimentally obtained stationary concentration ratio where $\phi_F{}^M$ and $\phi_F{}^C$ are the monomer and exciplex fluorescence quantum yields, respectively. The quantities $\tau_M{}^{-1}$

and τ_C^{-1} are summations of the various rate processes (other than equilibration) which deplete M* and MQ*, respectively.

Table I gives kinetic data for four exciplexes, two reactive (quantum yields for photoaddition, ϕ_R, are given in Table I) and two unreactive.[2,9] Complete discussion must await the full paper but several points appear clearly. (1) The radiative rates (k_F^C) for all four exciplexes are ca. 5 × 10^6 s^{-1}. Based on these and other published data,[4,10] a radiative rate of ca. 1-5 × 10^6 s^{-1} appears to be a useful rule of thumb both for excimers and for exciplexes possessing high charge-transfer stabilization, irrespective of their capability for forming stable photoproducts. (2) The reaction rates $(k_R^C = \phi_R \tau_C^{-1})$ vary by a factor of at least a thousand while the rates of radiationless decay $(k_D^C + k_{IS}^C)$ vary far less. It seems likely that the weakness or absence of exciplex emission in many reactive systems is a consequence of high reaction rates. (3) We have measured K_{eq} as a function of temperature for 9CNP⋯p-BA and find $\Delta H^\circ = -7.4$ kcal mol^{-1} and $\Delta S^\circ = -13.1$ cal mol^{-1} deg^{-1}, comparable with expectations based on Weller's finding[2] for arene-amine exciplexes. *Thermodynamic behavior thus appears to differ little between reactive and unreactive exciplexes.* Factors leading to formation of stable exciplexes are not necessarily those which cause exciplex collapse to *stable* products. It is possible that the failure to observe product formation in many systems where exciplexes can be observed reflects the instability with respect to starting materials of other metastable intermediates (e.g., biradicals) derived from exciplexes.[11] (4) Assumption of $\Delta S^\circ \simeq -15$ cal deg^{-1} mol^{-1} for those exciplexes where K_{eq} was not measured as a function of temperature leads to values of E_R, the repulsion energy[12] between unexcited M and Q at the equilibrium exciplex configuration, of 7.5-11.5 kcal mol^{-1}, again within the range of arene-amine exciplexes.

In summary, a combination of mode I and mode II experiments with steady-state quantum yield data provides virtually a complete kinetic analysis. Excited-state thermodynamic and kinetic parameters for reactive systems where reversion (k_{MC}) neither dominates nor is negligible seem accessible only with difficulty by the steady-state method owing to the possible temperature dependence[13] of k_R^C.
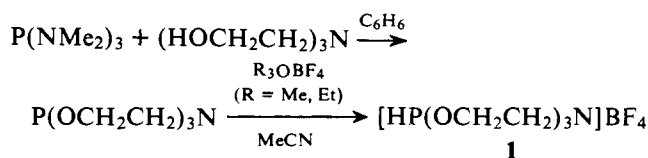
References and Notes

(1) (a) R. A. Caldwell and L. Smith, *J. Am. Chem. Soc.*, **96**, 2994 (1974); (b) D. Creed and R. A. Caldwell, *ibid.*, **96**, 7369 (1974).
(2) H. Knibbe, D. Rehm, and A. Weller, *Ber. Bunsenges. Phys. Chem.*, **73**, 839 (1969).
(3) Thermodynamic parameters for excimer formation have been extensively investigated. (a) E. Döller and Th. Förster, *Z. Phys. Chem. (Frankfurt am Main)*, **34**, 132 (1962); (b) J. B. Birks, D. J. Dyson, and I. H. Munro, *Proc. R. Soc. London, Ser. A*, **295**, 575 (1963); (c) B. Stevens and M. I. Ban, *Trans. Faraday Soc.*, **60**, 1515 (1963).
(4) B. Stevens, *Adv. Photochem.*, **8**, 161 (1971).
(5) (a) R. O. Loutfy, P. de Mayo, and M. F. Tchir, *J. Am. Chem. Soc.*, **91**, 3984 (1969); (b) O. L. Chapman and R. D. Lura, *ibid.*, **92**, 6352 (1970); (c) J. Saltiel, J. T. D'Agostino, O. L. Chapman, and R. D. Lura, *ibid.*, **93**, 2804 (1971); (d) T. Sugioka, C. Pac, and H. Sakurai, *Chem. Lett.*, 667 (1972).
(6) H. W. Offen and D. T. Phillips, *J. Chem. Phys.*, **48**, 2374 (1969).
(7) I. B. Berlman, "Handbook of Fluorescence Spectra of Aromatic Molecules", 2nd ed, Academic Press, New York, N.Y., 1971, p 356.
(8) Because of a long "tail" in the laser pulse ($\tau \approx 100$ ns, intensity about 2% of the total pulse intensity) the useful range of t is limited to that in which molecules excited in the laser tail make a negligible contribution to the total fluorescence. For 9-CNP⋯t-A, which has a short lifetime, meaningful results could not be obtained for $t \gtrsim 45$ ns. For the other systems studied, data were taken at least to $t \gtrsim 80$ ns.
(9) Y. Shirota, I. Tsushi, and H. Mikawa, *Bull. Chem. Soc. Jpn.*, **47**, 991

(1974).
(10) (a) N. Mataga, T. Okada, and N. Yamamota, *Chem. Phys. Lett.*, **1**, 119 (1967); (b) K. H. Grellmann and U. Suckow, *ibid.*, **32**, 250 (1975).
(11) I. E. Kochevar and P. J. Wagner, *J. Am. Chem. Soc.*, **94**, 3859 (1972); R. A. Caldwell, G. W. Sovocool, and R. P. Gajewski, *ibid.*, **95**, 2549 (1973).
(12) Derived from the expression[4] $h\nu_M - h\nu_C = -\Delta H^\circ + E_R$.
(13) D. Creed and R. A. Caldwell, unpublished work.
(14) Fellow of the Robert A. Welch Foundation.

David Creed,[14] Paul H. Wine[14]
Richard A. Caldwell, Lynn A. Melton

Institute for Chemical Sciences
The University of Texas at Dallas
Richardson, Texas 75080

Characterization and Molecular Structure of $[HP(OCH_2CH_2)_3N]BF_4$. Pentacoordination of Phosphorus

Sir:

While five-coordination in pentavalent phosphorus systems is profusely documented in the literature,[1] phosphonium cations have been found to be consistently four-coordinate. Here we report the characterization and molecular structure of **1** in which the presence of an N→P coordinate bond confers a trigonal bipyramidal geometry on the phosphorus atom. The second step of the reaction below invariably gives the expected alkyl phosphonium cation $RP(OR)_3^+$ with acylic

$$P(NMe_2)_3 + (HOCH_2CH_2)_3N \xrightarrow{C_6H_6}$$

$$P(OCH_2CH_2)_3N \xrightarrow[\text{MeCN}]{\substack{R_3OBF_4 \\ (R = Me, Et)}} [HP(OCH_2CH_2)_3N]BF_4$$
1

phosphite esters[2] or bicyclic phosphites such as $P(OCH_2)_3CMe$.[3] The abstraction of a proton which occurs with the present system[4] is highly suggestive of basicity enhancement of the phosphorus via nitrogen lone pair coordination.

In acetonitrile solution the presence of a $^1J_{PH}$ coupling of 791 Hz appearing in both the ^1H (δ, 6.03 d) and ^{31}P (δ, 20.2 d of mults[5]) NMR spectra of **1** is unusually low compared to those for $HP(OMe)_3^+$ (826.2 Hz)[6] and $HP(OCH_2)_3CMe^+$ (899.2 Hz)[6c,7] which can only be observed in strongly acidic media. This contrast indicates a comparatively low degree of s character in the P-H link of **1** consistent with a tricyclic structure in which the proton is located on the axis of a trigonal bipyramid.

To test this structural hypothesis, a crystal and molecular structure determination of **1** was undertaken by x-ray diffraction techniques. Preliminary examination of **1** showed that the crystals belong to the orthorhombic crystal class with $a = 12.784$ (6), $b = 9.320$ (4), and $c = 8.988$ (3) Å and four units of composition $HP(OCH_2CH_2)_3N \cdot BF_4$ per unit cell. Assignment of a space group was not unambiguous since the systematic extinctions ($0kl$ absent if $k + l = 2n + 1$, $h0l$ absent if $h = 2n + 1$) were consistent with both $Pna2_1$ and $Pnam$. In the latter space group the molecule would have to have a molecular mirror plane in the absence of disorder.

A total of 873 unique reflection intensities with $2\theta \leq 114°$ were measured using a computer controlled four-circle diffractometer and Cu K_α radiation (1.5418 Å). Of these, 615 were judged observed after correction for Lorentz, polarization, and background effects ($F_o \leq 3\sigma(F_o)$). Intensity statistics were not particularly helpful in deciding the space